

Stochastic cluster series expansion for quantum spin systems

Kim Louis and C. Gros

Fakultät 7, Theoretische Physik, University of the Saarland, 66041 Saarbrücken, Germany

(Received 4 June 2004; revised manuscript received 10 August 2004; published 30 September 2004)

In this paper we develop the stochastic cluster series expansion (SCSE) which is a (cluster) variant of the stochastic series expansion (SSE) method. For certain systems with longer-range interactions the SCSE is considerably more efficient than the standard implementation of the SSE, at low temperatures. As an application of this method we calculated the $T=0$ conductance for a linear Heisenberg chain with a (diagonal) next-nearest-neighbor interaction.

DOI: 10.1103/PhysRevB.70.100410

PACS number(s): 75.30.Gw, 75.10.Jm, 78.30.-j

I. INTRODUCTION

The development of efficient quantum Monte Carlo (QMC) methods with loop updates, like the loop algorithm¹ and the stochastic series expansion (SSE),²⁻⁵ has been a major advancement. They are very efficient for the anisotropic Heisenberg models, like the xxz chain, and can be generalized to more complicated Hamiltonians, but in some cases only with reduced performance.

Here we study the xxz chain with a diagonal next-nearest-neighbor interaction. This model is better suited for the description of fermionic systems, since it takes into account that the interaction (Coulomb repulsion) is long ranged. Furthermore, it is one of the simplest nonintegrable systems. Consequently, this model has attracted the attention of many authors.⁶⁻⁸

We find that a standard SSE implementation performs only poorly on our model system. The reason for this lies in the fact that a certain transition in the operator loop update—called “bounce”—is given a relatively large weight. Syljuåsen and Sandvik have shown that such a large bounce may affect the efficiency of the algorithm—especially at low temperatures. Hence, one should strive to find a way to reduce the bounce weight.

Here we report that a new implementation of the SSE algorithm, the stochastic cluster series expansion (SCSE), yields a considerably smaller bounce weight than the standard SSE, thus improving the efficiency considerably at low temperatures.

II. CONVENTIONAL SSE

We will now briefly discuss the conventional SSE implementation and point out its difficulties. Our model of interest is a frustrated chain with a diagonal next-nearest-neighbor interaction: (see Fig. 1),

$$H = \sum_n \left[\frac{J_x}{2} (S_n^+ S_{n+1}^- + S_n^- S_{n+1}^+) + J_z S_n^z S_{n+1}^z + J_{z2} S_n^z S_{n+2}^z \right]. \quad (1)$$

Note that only the interaction part is frustrated, such that a Monte Carlo simulation will not suffer from the sign problem. Following Ref. 2 we start by splitting the Hamiltonian

into a set of local operators, i.e., $H = \sum_{h \in \mathfrak{h}} h$ with $\mathfrak{h} = \{h_{n,n+1}^{(t)}, h_{n,n+2}^{(4)} : t=1,2,3; n \in \mathbb{N}\}$ and

$$h_{n,n+1}^{(1)} = J_x S_n^+ S_{n+1}^- / 2,$$

$$h_{n,n+1}^{(2)} = J_x S_n^- S_{n+1}^+ / 2,$$

$$h_{n,n+1}^{(3)} = C + J_z S_n^z S_{n+1}^z,$$

$$h_{n,n+2}^{(4)} = C_2 + J_{z2} S_n^z S_{n+2}^z, \quad (2)$$

where the constants C and C_2 are needed to ensure that all matrix elements between S^z -eigenbasis states are positive. Using the Taylor expansion, the partition function may be written as

$$Z = \sum_{M, \phi, \alpha} \frac{(-\beta)^M}{M!} \prod_{m=1}^M \langle \alpha_m, \phi(m) \alpha_{m+1} \rangle, \quad (3)$$

where $M \in \mathbb{N}$, $\phi: \{1, \dots, M\} \rightarrow \mathfrak{h}$, and the α_m run over all S^z -eigenbasis states with periodic boundary conditions $|\alpha_1\rangle = |\alpha_{M+1}\rangle$ along the imaginary-time axis. The factors $\langle \alpha_m, \phi(m) \alpha_{m+1} \rangle$ in Eq. (3) are called *plaquettes* and are non-negative due to (2). Hence, we can obtain the partition function by sampling the terms in Eq. (3) with their relative weight factors over all spin configurations $|\alpha_m\rangle$ and local operators $\phi(m) \in \mathfrak{h}$.

Since each operator $\phi(m)$ acts only on two sites, we may write

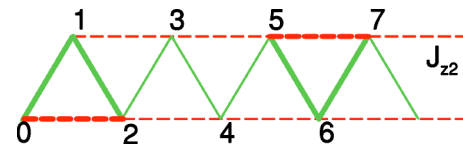


FIG. 1. (Color online) The model Hamiltonian that will be discussed in this paper. Solid lines indicate a full Heisenberg-like interaction between the sites; dashed lines stand for sites coupled only by a z - z term (Ising-like interaction). Two clusters, as defined in the text, are indicated by thicker lines.

$$W_{n_1, n_2}(s_{n_1}^m, s_{n_2}^m, s_{n_1}^{m+1}, s_{n_2}^{m+1}) := \langle \alpha_m, \phi(m) \alpha_{m+1} \rangle,$$

where $s_n^m = \langle \alpha_m, S_n^z \alpha_m \rangle$ are spin variables and W_{n_1, n_2} is given by the prefactors of (2). Note that because of translation invariance W_{n_1, n_2} depends actually only on $n_2 - n_1$. For brevity we will, in the sequel, denote the four arguments, which we call plaquette *legs*, by one super argument, which we call the plaquette *state*. The SSE knows two updates:

- (1) In the *diagonal update* an insertion/removal of one plaquette is considered.
- (2) The *loop update* (constructs and) flips a subset of the spin variables. Note that the resulting configuration must be allowed—that means it must have nonzero weight.

The loop update may be achieved step by step.² In each step we consider only one plaquette, whose state will be changed from i to j by flipping two legs l_i and l_j . The “incoming” leg l_i is given and we have to choose the “outgoing” leg l_j with a certain probability $p(i \rightarrow j, l_i, l_j)$. Of course, the probability for a transition $i \rightarrow j$ must be zero, if one of the states i or j has zero weight.

These probabilities—yet to be determined—will play a central role in what follows. Therefore, we will explain in detail how they are obtained.

They may equivalently be represented by $(2^4 \cdot 4) \times (2^4 \cdot 4)$ matrices a^{n_1, n_2} with entries

$$a_{(i, l_i)(j, l_j)}^{n_1, n_2} := p(i \rightarrow j, l_i, l_j) W_{n_1, n_2}(i).$$

The fact that the $p(i \rightarrow j, l_i, l_j)$ are probabilities imposes for each l_i and i the following conditions:

$$W_{n_1, n_2}(i) = \sum_{j, l_j} a_{(i, l_i)(j, l_j)}^{n_1, n_2}. \quad (4)$$

The detailed balance condition is satisfied if the matrices a^{n_1, n_2} are symmetric.

Closer inspection shows that the matrices a^{n_1, n_2} are block diagonal, where the dimension of the blocks d equals half the number of allowed plaquette states. Hence, if $n_2 - n_1 = 1$, we have $d = 3$, whereas $d = 2$ for $n_2 - n_1 = 2$.

All the elements in one single block of a^{n_1, n_2} differ in at least one state index. Hence, we may drop the leg indices l_i and l_j without causing ambiguities. Moreover, we will also omit the explicit indication of the site indices n_1 and n_2 in a and W .

For the blocks of length 3 a formal solution for the non-diagonal entries a_{ij} , which meets detailed balance and Eq. (4), can easily be stated,⁵

$$a_{ij} = [W(i) + W(j) - W(k)]/2 + [a_{kk} - a_{ii} - a_{jj}]/2, \quad (5)$$

where k is the third plaquette state in the same block of a as i and j . One sees that the diagonal entries of the matrices a remain free, apart from the final restriction that all probabilities (entries of a) need to be positive. Reference 5 found that the most favorable among all possible solutions to Eq. (4) is the one where the diagonal entries (called bounces) are minimal.

If $d = 3$ all bounce weights may be put to zero for a wide parameter range,⁵ but when $d = 2$, Eq. (4) dictates one of the two bounces a_{ii} and a_{jj} to be equal to $|W(i) - W(j)| = J_z/2$, a situation which is far from optimal.

III. CLUSTER VARIANT (SCSE)

The problem with the SSE method is that some plaquettes—associated with operators $h^{(4)}$ —have only four allowed (diagonal) states. This can be avoided by using a different splitting of the Hamiltonian. We now introduce the stochastic *cluster* series expansion (SCSE). In the case of the frustrated chain we split the Hamiltonian (1) not into two- but three-sites operators (see Fig. 1),

$$h_{n, n+1, n+2}^{(1)} = J_x S_n^+ S_{n+1}^- / 4 = (h_{n, n+1, n+2}^{(2)})^\dagger,$$

$$h_{n, n+1, n+2}^{(3)} = J_x S_{n+1}^+ S_{n+2}^- / 4 = (h_{n, n+1, n+2}^{(4)})^\dagger,$$

$$h_{n, n+1, n+2}^{(5)} = J_z/2 (S_n^z S_{n+1}^z + S_{n+1}^z S_{n+2}^z) + J_{z2} S_n^z S_{n+2}^z + C.$$

Note the factor $1/4$ instead of $1/2$ for $h^{(t)}$ with $t = 1, 2, 3, 4$. It stems from the fact that each nondiagonal operator is “distributed” between two clusters.

The diagonal update and loop construction remain unchanged with respect to the SSE. In the loop update the only difference is that W is now a function of six variables. Let us now turn to the matrix a . The transitions of the form $h^{(t)} \rightarrow h^{(r)}$, when $t \in \{1, 2\}$ and $r \in \{3, 4\}$, will be ruled out from the beginning (for simplicity and because we do not expect that they will give assistance in minimizing the bounce). All other transitions may have positive probability.

For a given plaquette — associated with an operator $h^{(t)}$ — and a given ingoing leg, whose site index is $n_i \in \{n, n+1, n+2\}$, we can directly tell the dimension of the corresponding block of a and give a solution for its entries. There are three cases to be considered:

(1) For $t = 1, 2$ and $n_i = n+2$ (or $t = 3, 4$ and $n_i = n$) we get only two equations from Eq. (4). Since both plaquette states [corresponding to nondiagonal $h^{(t)}$] have equal weights, we can put the bounce weight to zero. The proceeding of the loop is then deterministic.

(2) Otherwise if $(t = 5, n_i \neq n+1)$ or $(t \neq 5, n_i = n+1)$ we have to consider three equations which may be treated as in the SSE [see Eq. (5)].

(3) In the remaining cases we need to solve a subsystem of Eq. (4) of not less than four equations, (see Fig. 2). Among the four plaquette states involved in this block we find two states corresponding to nondiagonal $h^{(t)}$ —which we call i_n and j_n . From Fig. 2 we infer that if i_n corresponds to $t \in \{1, 2\}$, j_n corresponds to $t \in \{3, 4\}$, and vice versa. The remaining two states correspond to diagonal operators; we call them i_d and j_d . The entries of a are given by

$$a_{i_n, i_d} = \max\{[W(i_d)/2 + W(i_n) - W(j_d)]/2, 0\},$$

$$a_{i_n, j_d} = \min\{[W(j_d)/2 + W(i_n) - W(i_d)]/2, W(i_n)\},$$

$$a_{i_d, j_d} = \min\{[W(i_d) + W(j_d) - 2W(i_n)]/2, W(i_d)\},$$

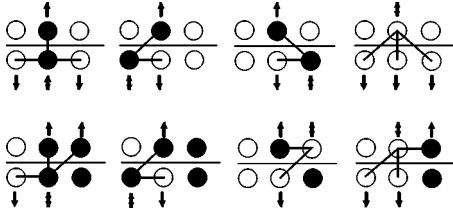


FIG. 2. Pictorial representation of the plaquettes, similar to the one used in Ref. 5. The operators are represented by a horizontal central bar with six circles which stand for the six plaquette legs. The filled and empty circles mean opposite spin directions. Shown are two examples of a block of dimension 4 of Eq. (4). (The other blocks of the same dimension may be obtained by obvious symmetry transformations.) The possible (local) loop courses are indicated by lines and arrows (in- and outgoing legs). The reader may convince oneself that upon flipping the two spins belonging to a loop segment and interchanging in- and outgoing legs one diagram becomes another; the weights are then related by detailed balance.

$$a_{j_d j_d} = \max\{0, W(j_d) - W(i_d) - 2W(i_n)\},$$

$$a_{j_n k} = a_{i_n k}, \quad k = i_d, j_d.$$

Note that we assumed $W(i_d) \leq W(j_d)$ and exploited $W(i_n) = W(j_n)$. With this choice only one diagonal entry (namely, $a_{j_d j_d}$) may be non-negative. To be concrete, only the situation depicted in the upper part of Fig. 2 admits $a_{j_d j_d} = (J_z - J_x)/2 > 0$, if $J_z > J_x$.

The SCSE is more intricate (one has to consider several cases separately) and the bounce cannot always be avoided, but there is a considerable improvement (at low temperatures) with respect to the SSE.

IV. NUMERICAL RESULTS

In this paper we use the method proposed in Ref. 9 to calculate the conductance for the Hamiltonian (1). We evaluate the expression,

$$g(\omega_M) = -\omega_M/\hbar \int_0^{\hbar\beta} \cos(\omega_M \tau) \langle P_x P_y(i\tau) \rangle d\tau \quad (6)$$

at the Matsubara frequencies $\omega_M = 2\pi M(\beta\hbar)^{-1}$, $M \in \mathbb{N}$. The conductance is obtained by extrapolating $g(\omega)$ from the Matsubara frequencies to $\omega=0$. The operators in Eq. (6) are given by (e is the charge unit) $P_x = e \sum_{n>x} S_n^z$. The two parameters x and y represent essentially the position of the current measurement and of the voltage drop; the value of $g(\omega=0)$ depends on neither of them.

To illustrate the improvement gained by introducing SCSE we performed for a special choice of parameters ($J_z = 2J_{z2}$) simulations of $g(\omega_M)$. In Fig. 3 we plotted the ratio of the consumed time along with the ratio of the mean statistical error in $g(\omega_M)$ (for $M=1, \dots, 10$). The SSE is slightly faster (about 80%), but while the statistical error grows quadratically with J_z for SSE, it grows more modestly for the SCSE.

Since the statistical error ratio $\epsilon^{(SSE)}/\epsilon^{(SCSE)}$, (the superscript indicates the method) increases with J_z , we may use

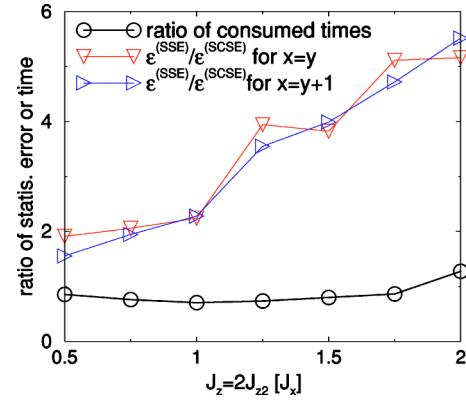


FIG. 3. (Color online) We compare simulations ($J_z = 2J_{z2}$, 192 sites, $T = 0.01J_x/k_B$, 2×10^4 MC sweeps) for SSE and SCSE. Shown is the ratio of the time consumed by the SSE and SCSE simulations, as well as the ratio of the mean (over the first ten Matsubara frequencies) statistical error ϵ of SSE and SCSE. $x = N/2$ and y are defined in Eq. (6).

the gain in performance to reach higher values of J_z with the SCSE. We find by using a quadratic fit for the errors $\epsilon^{(SSE)}(J_z)$ and $\epsilon^{(SCSE)}(J_z)$, for $x = y + 1$,

$$[\epsilon^{(SCSE)}]^{-1} [\epsilon^{(SSE)}(J_z)] \approx 3J_z^2,$$

indicating that the SCSE gives access to an (at least) three times larger J_z interval than the SSE.

We also performed simulations of the susceptibility for a two-dimensional analog of our model on a 16×16 square lattice. We report that the SCSE gives a three- to tenfold smaller statistical error than the SSE when $J_z = 3J_x = 2J_{z2}$, $0.05J_x \leq k_B T \leq 0.5J_x$, whereas at $J_{z2} < J_x$ the SSE is slightly more efficient. $[\epsilon^{(SSE)}/\epsilon^{(SCSE)}]$ actually increases from 3 to 10 as $k_B T$ decreases from $0.5J_x$ to $0.05J_x$.

V. FRUSTRATED SYSTEM

Using the Lanczos method Zhuravlev, Katsnelson, and co-workers⁸ obtained a very complete picture of the frustrated system given by the Hamiltonian (1). They setup a low-temperature phase diagram with two gapped and a gapless phase. In the gapless phase the system is, for a large range of parameters, very well described by the Luttinger liquid picture.⁸ In Fig. 4 $g(\omega=0)$ —extrapolated by a quadratic fit—is plotted versus J_{z2} for various $J_z < J_x$. For this region in parameter space, Ref. 8 finds a phase boundary between the gapless and the gapped phase at $J_{z2} = J_x$.

In a Luttinger liquid the conductance equals the Luttinger parameter^{9–11} and may hence be viewed as an effective interaction. Since J_{z2} mediates a nearest-neighbor attraction and thereby reduces the effective interaction, the conductance first grows with J_{z2} and then assumes its maximum approximately when $2J_{z2} = J_z$ is satisfied. We see that within error bars the conductance does not vary on the phase boundary.

As we work at a finite temperature of $k_B T = 0.01J_x$, the conductance goes smoothly to zero in the gapped phase, such that a determination of the phase, boundary from Fig. 4 becomes difficult.

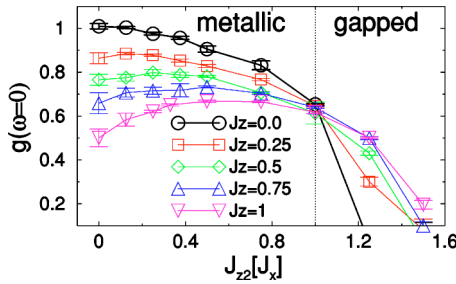


FIG. 4. (Color online) Conductance of the Heisenberg chain (400 sites, $T=0.01J_x/k_B$) with next-nearest-neighbor interaction J_{z2} . The phase boundary from Ref. 8 is displayed. (We use open boundary conditions, 2×10^5 MC sweeps.)

A remarkable fact of the phase diagram in Ref. 8 is the fact that the gapless phase is not bounded in parameter space; it contains, e.g., the line with $2J_{z2}=J_z$. It is therefore interesting to study the behavior of the conductance on this line. However, if we increase J_z and J_{z2} simulating the conductance becomes more difficult. (The statistical error grows.)

Only the SCSE allows us to compute the conductance for as large interaction values as $J_z=5, J_{z2}=2.5$. The conductance is plotted in Fig. 5. Besides the statistical error we have an extrapolation error depending on our extrapolation scheme. In Fig. 5 we compared two schemes: a quadratic fit to the first three Matsubara frequencies and a linear fit from the first six Matsubara frequencies. The former should give a smaller extrapolation error, but it enhances the statistical error of $g(\omega)$. The latter has a larger extrapolation error, but it suppresses the statistical error of $g(\omega)$. For small parameters the two fits almost coincide. But for larger parameter values—when the statistical error increases—the quadratic fit starts to fluctuate.

For this system the Drude weight D and the susceptibility χ at $T=0$ may be obtained by exact diagonalization.⁸ The

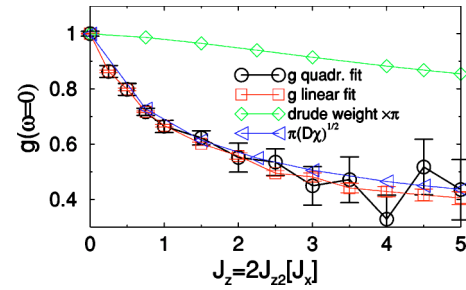


FIG. 5. (Color online) Conductance of the Heisenberg chain (400 sites, $T=0.01J_x/k_B$) with next-nearest-neighbor interaction J_{z2} along the line in parameter space where $2J_{z2}=J_z$. (Circle) quadratic extrapolation from the first three Matsubara frequencies, (square) linear extrapolation from the first six Matsubara frequencies. (We use OBC's, 2×10^5 MC sweeps.) For comparison exact diagonalization results are given.

same is true for the conductance via the relation $g=\pi\sqrt{D}\chi$ valid for a Luttinger liquid.^{10,12} Figure 5 provides also the exact diagonalization data showing good agreement with the SCSE data within error bars.

VI. CONCLUSION

In this communication we showed that the performance of the SSE can be substantially improved by selecting a different splitting of the Hamiltonian. As a test we considered here a spin model with a frustrated interaction part. We have reported here an appreciable gain in performance for this model in one dimensions, in two dimensions our preliminary data show a dramatic improvement for certain parameters, such that our method would allow the exploration of a portion of phase space inaccessible with SSE alone. Our method can also be applied to further systems, e.g., the problem of Coulomb drag of the Hubbard model where we also found an increased performance.

¹H. G. Evertz, G. Lana, and M. Marcu, Phys. Rev. Lett. **70**, 875 (1993).

²A. W. Sandvik, Phys. Rev. B **59**, R14 157 (1999).

³A. Dorneich and M. Troyer, Phys. Rev. E **64**, 066701 (2001).

⁴A. W. Sandvik and J. Kurkijärvi, Phys. Rev. B **43**, 5950 (1991); A. W. Sandvik, J. Phys. A **25**, 3667 (1992).

⁵O. F. Syljuåsen and A. W. Sandvik, Phys. Rev. E **66**, 046701 (2002).

⁶X. Zotos and P. Prelovšek, Phys. Rev. B **53**, 983 (1996).

⁷B. N. Narozhny, A. J. Millis, and N. Andrei, Phys. Rev. B **58**, R2921 (1998).

⁸A. K. Zhuravlev, M. I. Katsnelson, and A. V. Trefilov, Phys. Rev. B **56**, 12 939 (1997); A. K. Zhuravlev and M. I. Katsnelson, *ibid.* **61**, 15 534 (2000); A. K. Zhuravlev and M. I. Katsnelson, *ibid.* **64**, 033102 (2001).

⁹K. Louis and C. Gros, Phys. Rev. B **68**, 184424 (2003).

¹⁰W. Apel and T. M. Rice, Phys. Rev. B **26**, 7063 (1982).

¹¹T. Giamarchi and H. J. Schulz, Phys. Rev. B **37**, 325 (1988).

¹²H. J. Schulz, Los Alamos Meeting on Strongly Correlated Electron Systems, Los Alamos, 1993 (unpublished); cond-mat/9412036.